2019

Dissecting a Role for Polyamines in Rift Valley Fever Virus Infection

Vincent Mastrodomenico

LOYOLA UNIVERSITY CHICAGO

DISSECTING A ROLE FOR POLYAMINES IN RIFT VALLEY FEVER VIRUS INFECTION

A THESIS SUBMITTED TO

THE FACULTY OF THE GRADUATE SCHOOL

IN CANDIDACY FOR THE DEGREE OF

MASTER OF SCIENCE

PROGRAM IN MICROBIOLOGY AND IMMUNOLOGY

BY

VINCENT MASTRODOMENICO

CHICAGO, ILLINOIS

JUNE 2019

ACKNOWLEDMENTS

I would like to thank Dr. Bryan Mounce, PhD, for being an exemplary mentor throughout my time at Loyola. It is with his guidance and unique perspective that I have learned to be proud of my milestones and overcome any obstacle in my path. I would also like to thank my entire lab, but especially Patrick Tate, Courtney Dial, and Tom Kicmal. You all have been with me every step of the way, and I could not be more grateful for all your help.

I would also like to thank the members of my thesis committee (Dr. Susan Baker and Dr. Yee Ling Wu) for questioning me, challenging me, and not only being incredibly supportive, but also motivating me to become a better scientist.

Lastly, I would like to thank my friends and family for providing me with love and support through all the difficulties that graduate students encounter. I would particularly like to thank my undergraduate mentor, Dr. Zachary Pratt, for being the inspiration behind my interest in biomedical science in the first place.

TABLE OF CONTENTS

LIST OF FIGURES

LIST OF TABLES

LIST OF ABBREVIATIONS

Rift Valley fever virus	RVFV
Rift Valley fever	RVF
La Crosse virus	LACV
Zika virus	ZIKV
Viral RNA	vRNA
Complementary RNA	cRNA
Ornithine decarboxylase	ODC1
Spermidine synthase	SRM
Spermine synthase	SMS
Spermine oxidase	SMOX
Spermidine/spermine acetyltransferase	SAT1
Polyamine oxidase	PAOX
Herpes simplex virus 1	HSV1
Vaccinia virus	VACV
Human cytomegalovirus	HCMV
Human immunodeficiency virus	HIV1
Eukaryotic translation initiation factor 5A	eIF5A
Semiliki Forest virus	SFV
Difluoromethylornithine	DFMO

N1,N11-diethylnorospermine	DENSpm
Keystone virus	KEYV
Thin layer chromatography	TLC
Multiplicity of Infection	MOI
Quantitative Real Time PCR	qRT-PCR
Plaque forming unit	PFU
Encephalomyocarditis virus	EMCV
Newcastle disease virus	NDV
Coxsackie B3 virus	CVB3

ABSTRACT

Bunyaviruses are emerging viral pathogens that cause encephalitis, hemorrhagic fevers, and meningitis. Rift Valley fever virus is a particularly devastating bunyavirus, infecting both humans and livestock with significant morbidity and mortality. By coordinating several host and viral processes Rift Valley fever virus is able to produce infectious virions. Polyamines are small, positively-charged host-derived molecules that play diverse roles in human cells and in infection. We previously demonstrated that polyamines are crucial for RNA viruses; however, the mechanisms by which polyamines function remain unknown. Here, we investigated polyamines' role in the replication of the Rift Valley fever virus (vaccine strain MP-12). We found that polyamine depletion did not impact viral RNA or protein accumulation. Viral particles demonstrated no change in morphology, size, or density, however, targeting polyamines significantly reduced viral titers. In sum, polyamine depletion results in the accumulation of noninfectious particles which has important implications for targeting polyamines therapeutically, as well as enhancing vaccine strategies.

CHAPTER 1: BACKGROUND

Review of Literature

Rift Valley Fever Virus: an Overview

The sudden emergence of viral pathogens is of great concern since they devastate both human and veterinary health (1). The National Institute of Allergy and Infectious Disease categorizes emerging infectious diseases by the organism/pathogen which possess the highest health risk to national security and public health. Category A pathogens are of the highest priority since they can easily be transmitted, result in high morbidity rates, cause mass social disruption, and require immediate action from healthcare professionals (2). Within this category are Bunyaviruses (2). Bunyaviruses are of particular interest because this viral family is the largest family with more than 350 member viruses (3). With so many viruses in this family, the potential for outbreaks is great and current reports have noted a recent outbreak of Rift Valley fever, caused by Rift Valley fever virus (RVFV)(4, 5).

RVFV is currently restricted to Africa and the Middle East. The disease was first identified and characterized in 1930 by Dauney et al. (6) in Kenya. From its identification, it remained a serious health concern for in East Africa and subsequently, the first major outbreak was reported in 1977 in Egypt (7). The second major outbreak occurred in 2000 moving from East Africa to Saudi Arabia and Yemen in the Arabian Peninsula (7, 8). Outbreaks continued in Kenya, Somalia, Tanzania in 2007, Sudan in 2008 and 2010, and more recently in Uganda and Niger in 2016 (4, 7). RVFV

appears to have excellent potential for spreading to new areas and therefore must be further studied to persevere human and animal health.

RVFV, the causative agent of Rift Valley fever, normally causes an acute febrile illness which can escalate and cause severe disease including encephalitis, hemorrhagic fever in humans, as well as spontaneous abortion in domesticated animals (7, 9). RVFV is an arthropod-borne virus (arbovirus) that infects a wide range of wild and domestic vertebrate species, mainly ruminants such as sheep, cattle, and goats (10, 11). The primary and secondary vectors of RVFV are the *Aedes* and *Culex* mosquitos(12). The RVFV transmission cycle, summarized in Figure 1, is maintained through horizontal transmission, direct contact transmission with infected tissue and fluid, and suspected vertical transmission between mosquitos and ruminants with humans being considered as the dead-end host (11, 13).

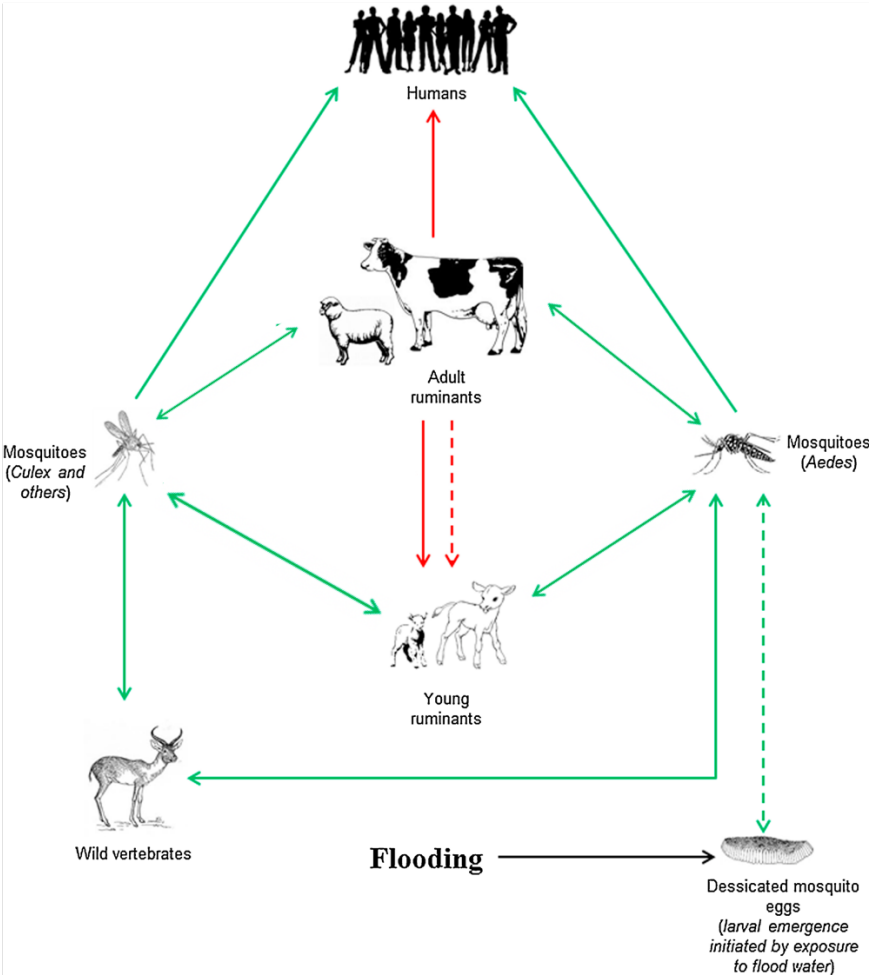

Figure 1. Transmission Cycle of RVFV.
Arrows represent transmission direction. Solid green lines represent established routes of horizontal transmission from collected data. Solid red lines represent established routes of direct contact transmission from infected tissue and fluids. Dotted lines, both green and red, are suspected routes of vertical transmission but current data is insufficient. Adapted and modified image from (11).

Outbreaks of RVFV often force a heavy restriction on livestock movement to prevent spread, causing massive economic loss. In addition, a major concern for society would be the continued spread of RVFV and the spread of other bunyaviruses. A distantly related bunyavirus, La Crosse virus (LACV) also causes encephalitis following infection transmitted by a mosquito bite and is primarily localized to midwestern and mid-Atlantic states of the USA (14, 15). Further, the rapid dissemination of several other

arboviruses like chikungunya (16) and Zika (17) viruses (ZIKV) demonstrate the extreme epidemic potential of arboviruses, including bunyaviruses.

Rift Valley Fever Virus Structure, Life Cycle, and Production

To remain pathogenic, viruses must maintain infectivity following successful replication of their viral genomes (Figure 2). RVFV has a tripartite negative-stranded RNA genome which is comprised of small (S), medium (M), and large (L) segments(18). The S segment (1.7 kB) is of ambisense orientation consisting of 2 proteins: the nucleoprotein (N) and a nonstructural protein (NSs protein). The M segment (3.2 kB) encodes the glycoproteins, Gn and Gc, and a 78 kD protein with an unknown function. Lastly, the L segment (6.4 kB) encodes the RNA-dependent RNA polymerase (L protein)(18, 19).

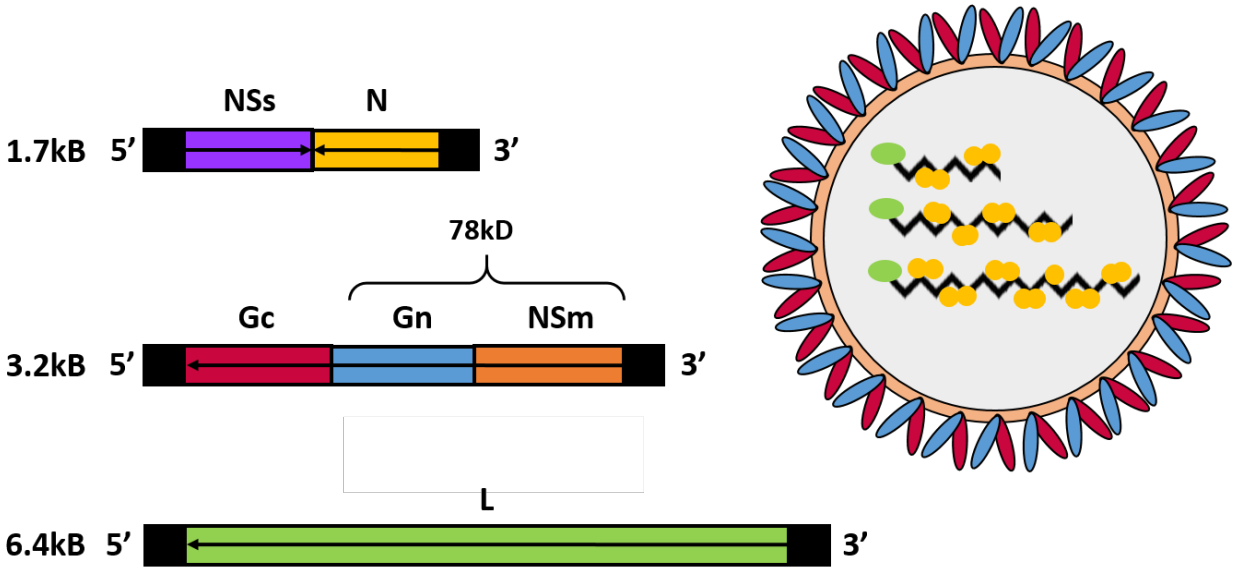

Figure 2. Schematic Diagram of Rift Valley Fever Virus
The panel above illustrates the RVFV virion containing the S, M, and L RNA segments in addition to the glycoproteins incorporated in the envelope. The arrows indicate the direction of viral protein production. The viral proteins include the polymerase (L), glycoproteins (Gc and Gn), Nonstructural M protein (NSm), Nonstructural S protein (NSs) and nucleoprotein (N).

All viruses must complete an entire replication cycle in host cells to produce viable progeny. Figure 3 depicts the viral life cycle of RVFV. It first attaches to an unknown host cell receptor mediated by interactions of viral glycoproteins and host proteins. Through receptor-mediated endocytosis, the virus enters the cell in an early endosome. The virion will fuse to the endosomal membranes upon acidification and undergoes viral uncoating. The release of the viral RNA (vRNA) into the cytoplasm begins primary transcription of the vRNA to produce complementary RNA (cRNA) for translation and additional transcription. Viral proteins are produced and are transported to the ER-Golgi complex where encapsidation occurs followed by egress at the plasma membrane (20). These several factors (shown in Figure 2 and Figure 3) are essential for RVFV and contribute to the infectivity of progeny bunyaviruses (21), inclusion of replicative proteins (L and N proteins), and successful envelopment.

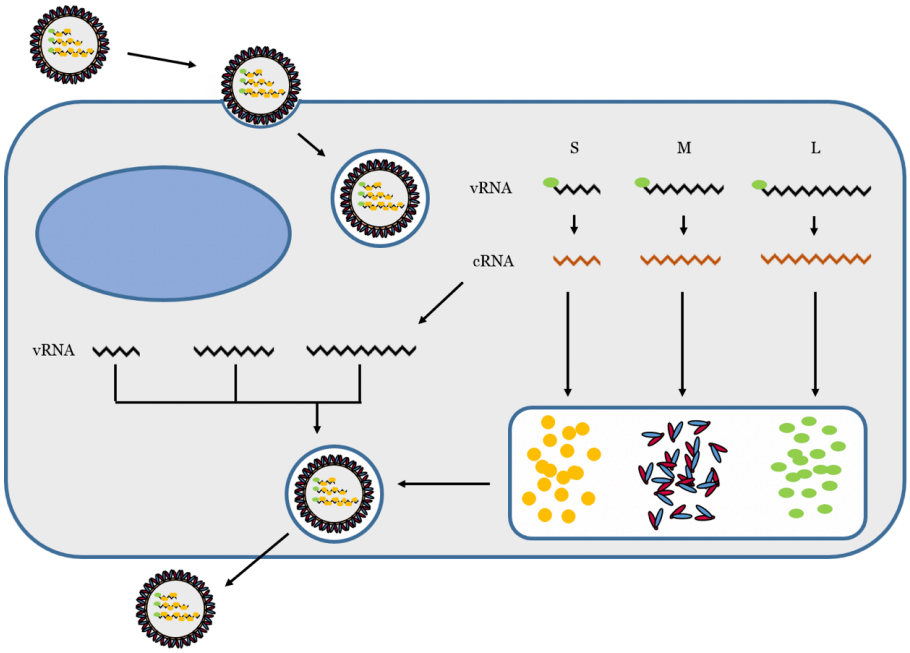

Figure 3. Bunyavirus Replication Cycle.
The viral life cycle beings with attachment of virus to a host receptor. The virus undergoes receptor mediated endocytosis and enters the cell. Uncoating follows upon acidification and fusion with the endosome. Transcription of the viral RNA begins to produce complementary S, M, and L segments. Transcription of viral RNA continues in addition to translation of viral proteins. The proteins are transported to the ER-Golgi complex for further synthesis and encapsidation. Maturation of the virion occurs and egresses from the plasma membrane.

It is important to note that the proportion of infectious virions versus noninfectious particles in RNA virus infection is low, with noninfectious particles outnumbering infectious particles by 100- to 1000-fold (22). An example of this phenomenon is for Bunyamwera virus, a related bunyavirus (22). The factors contributing to this ratio are multifactorial, but have important implications for infection and pathogenesis (23). The noninfectious particles can serve as decoys from immune system neutralization, enhancing infection by infectious particles (24, 25). In contrast, noninfectious particles can interfere with productive infection, by binding cellular receptors or usurping cellular and viral machinery from infectious viruses (26). Defective genomes play a role in

pathogenesis; for example, paramyxoviruses persist in their hosts by maintaining a balance of replication and apoptosis, which is modulated by defective viruses (27). Additionally, arthropod-borne viruses persist in their hosts at least partially through defective viral genomes feeding into host immune defenses such as the RNAi pathway (28). The precise mechanisms by which viruses produce defective genomes remains to be understood for several viral families. Importantly, the cellular contribution to this ratio of infectious-to-noninfectious virus is unclear.

Role of Polyamines in Viral Infection

Polyamines are small, positively-charged molecules found abundantly in all cells. Mammalian cells exclusively synthesize three biogenic polyamines(29). Within a cell, arginine is converted to ornithine which is the first step in this synthetic pathway, shown in Figure 4. Ornithine is converted into the polyamine putrescine via the gatekeeping enzyme of the pathway, ornithine decarboxylase 1 (ODC1). Following synthesis of putrescine, an enzyme, spermidine synthase (SRM), coverts putrescine to spermidine. Spermidine is then converted to spermine with spermine synthase (SMS). Subsequently, spermine can be converted back to spermidine via spermine oxidase (SMOX) and putrescine via spermidine/spermine acetyltransferase (SAT1) and polyamine oxidase (PAOX)(29). The polyamine synthesis pathway is important for many cellular processes, such as cell cycling, nucleic acid binding, and altering membrane fluidity (30–32).

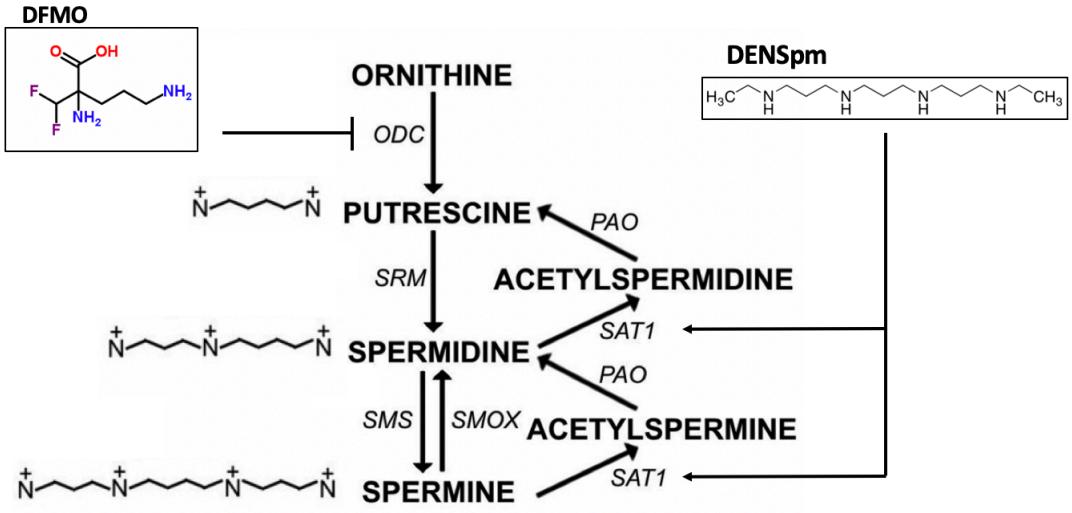

Figure 4. Biosynthesis Pathway of Polyamines and Drug Inhibitors
Polyamine synthesis begins with arginine being converted into ornithine. ODC1, the rate-limiting enzyme, converts ornithine to putrescine. Putrescine is converted to spermidine via SRM. Spermidine is converted to spermine via SMS and converted back via SMOX. Spermine and spermidine can be acetylated by SAT1 and converted back to putrescine via PAO. DFMO is an irreversible inhibitor to ODC1 preventing polyamine synthesis and DENSpm activates SAT1 to acetylate spermidine and spermine which will convert back to putrescine or are exported out of the cell. Image adapted and modified from (33).

With the abundance of polyamines being utilized in cells for diverse processes, it is not surprising that viruses use polyamines for their own replication. Viruses like herpes simplex 1 (HSV1), vaccinia virus (VACV), and human cytomegalovirus (HCMV) have been reported to contain polyamines within the virion and are involved in viral packaging (34–36). Ebolavirus, Marburgvirus, and human immunodeficiency virus (HIV-1) utilize polyamines in translation through the hypusination of eukaryotic translation initiation factor 5A (eIF5A) (37–39). Additionally, the depletion of polyamines reduces viral titers of many RNA viruses and was first demonstrated with an infrequent human pathogen found in the alphavirus family, Semliki Forest virus (SFV) (29, 40). The polyamine pathway has been considered a pharmacological target for numerous

cancers and targeting this pathway could be a feasible way to reduce various viral infections. An FDA approved drug, difluormethylornithine (DFMO) is a specific, nontoxic inhibitor of ODC1 (Figure 4). By reducing cellular or organismal polyamine levels, it is used to target diverse cancer types and is the primary treatment for trypanosomiasis (41, 42). Despite a reliance on polyamines for cellular growth and division, polyamine-depleted mammalian cells maintain viability without significant toxicity (43, 44). Additionally, *N*1,*N*11-diethylnorspermine (DENSpm) is another pharmacological agent with therapeutic potential. Treatment of cells with DENSpm results in the upregulation of SAT1 and subsequent acetylation of spermidine and spermine(29). This acetylation results in an increase of reconverted putrescine or export of these polyamines from the cell (29, 45, 46) (Figure 4). These pharmacological agents are promising therapeutics, and they also provide valuable tools to study the roles of polyamines in virus infection. It is not known whether bunyaviruses utilize polyamines and with these pharmalogical agents, we can assess whether these drugs work against RVFV.

Aims and Hypothesis

Recent studies demonstrated that RNA viruses rely on polyamines for replication (29). Initially, it was found that positive-stranded RNA viruses, like chikungunya and Zika virus, required polyamines for translation of the viral polyprotein as well as viral RNA-dependent RNA polymerase activity (47). Olsen *et al*. uncovered that Ebola virus relies on polyamines for translation of viral proteins through the spermidine metabolite hypusine (37–39). It was further shown that a range of RNA viruses rely on polyamines for replication, both *in vitro* and *in vivo* (48). Prior work has established a role for

polyamines in virion packaging of nucleic acid in several DNA viruses (34–36). RNA viruses, in contrast, were characterized to package negligible levels of polyamines (49). Additionally, Mounce et al. highlighted the importance of the polyamine biosynthetic pathway as a target in the development of future antivirals. Upon depletion of polyamines through different pharmalogical agents that target the key players in polyamine biosynthesis, viral replication was severely limited (48). Currently, little is understood about polyamines in the viral lifecycle of bunyaviruses like RVFV. The goal of this proposal is to determine how polyamines may be involved in virus production and how they modulate RVFV infectivity.

In AIM 1, we examined whether polyamine depletion alters RVFV infection. I hypothesized that RVFV, like other RNA viruses, would be affected by polyamine depletion. Results from this aim establish the importance of polyamines for RVFV and to identify where polyamines may play a role in the RVFV replication cycle.

In AIM 2, I assessed virion production and composition of RVFV from cells with and without polyamines. I hypothesized that polyamines are essential for proper production of infectious RVFV; thus, in the absence of polyamines, infectious virion composition is compromised. The goal of this aim was to investigate RFVF genome abundance, size, and functionality in the presence of polyamine depleting drugs.

In AIM 3, I proposed that polyamines contribute to the gross architecture of RVFV. I hypothesized that RVFV utilizes polyamines for proper virion maturation like VACV and HSV1. The goal of this aim was to define the direct or indirect impact on the physical properties of RVFV in the presence of polyamine depleting drugs.

The data generated from these aims demonstrated that RVFV uses polyamines for its replication. Although there was no change in morphology and viral protein levels were unchanged, we see an increase in RVFV genome-to-PFU ratio and a reduction in viral titer.

CHAPTER 2: MATERIALS AND METHODS

Cell Culture

Cells were maintained at 37ºC in 5% CO_2, in Dulbecco's modified Eagle's medium (DMEM; Life Technologies) with bovine serum and penicillin-streptomycin. Vero cells (BEI Resources) were supplemented with 10% new-born calf serum (NBCS; Thermo-Fischer) and Huh7 cells, kindly provided by Dr. Susan Uprichard, were supplemented with 10% fetal bovine serum (FBS; Thermo-Fischer). THP1 cells were donated by Dr. Makio Iwashima and maintained in RPMI (Thermo-Fischer) supplemented with 2% FBS and beta-mercaptoethanol (BME, 50mM; Thermo-Fischer). THP1's were differentiated with phorbol 12-myristate 13-acetate (PMA, 100 pg/ mL; Thermo-Fischer). RAW264.1 macrophages were provided by Dr. Katherine Knight and maintained in 2% FBS.

Drug Treatment

Difluoromethylornithine (DFMO; TargetMol) and N1,N11-Diethylnorspermine (DENSpm; Santa Cruz Biotechnology) were diluted to 100x solution (100mM and 10mM, respectively) in sterile water. For DFMO treatments, cells were trypsinized (Zymo Research) and reseeded with fresh medium supplemented with 2% serum. Following overnight attachment, cells were treated with 100 µM, 500 µM, 1 mM, or 5 mM DFMO. Cells were incubated with DFMO for 96 hours to allow for depletion of polyamines in Huh7 cells. For DENSpm treatment, cells were treated with 100 nM, 1

μM, 10 μM, 100 μM, and 1mM 16 hours prior to infection. During infection, media was cleared and saved from the cells. The same medium containing DFMO and DENSpm was then used to replenish the cells following infection. Cells were incubated at the appropriate temperature for the duration of the infection.

Infection and Enumeration of Viral Titers

MP-12 (50), LACV, and KEYV were derived from the first passage of virus in Huh7 cells. ZIKV (MR766) was derived from the first passage of virus in Vero cells. CVB3 (Nancy strain) was derived from the first passage of virus in HeLa cells. ZIKV, LACV, and, KEYV were obtained from Biodefense and Emerging Infections (BEI) Research Resources. For all infections, DFMO and DENSpm were maintained throughout infection as designated. Viral stocks were maintained at -80ºC. For infection, virus was diluted in serum-free DMEM for a multiplicity of infection (MOI) of 0.1 on Huh7 cells, unless otherwise indicated. Viral inoculum was overlain on cells for 10 to 30 minutes, and the cells were washed with PBS before replenishment of media. Supernatants were collected from MP-12, LACV, KEYV, ZIKV, and CVB3 24 hpi. Dilutions of cell supernatant were prepared in serum-free DMEM and used to inoculate confluent monolayer of Vero cells for 10 to 15 min at 37ºC. Cells were overlain with 0.8% agarose in DMEM containing 2% NBCS. CVB3 samples incubated for 2 days, MP-12, ZIKV, and LACV samples incubated for 3 days and KEYV samples incubated for 5 days at 37ºC. Following appropriate incubation, cells were fixed with 4% formalin and revealed with crystal violet solution (10% crystal violet; Sigma-Aldrich). Plaques

were enumerated and used to back-calculate the number of plaque forming units (pfu) per milliliter of collected volume.

Thin Layer Chromatography Determination of Polyamines

Polyamines were separated by thin-layer chromatography as previously described (Madhubala, 1998). For all samples, cells were treated as described prior to being trypsinized and centrifuged. Pellets were washed with PBS and then resuspended in 200 uL 2% perchloric acid. Samples were then incubated overnight at 4ºC. 200 uL of supernatant was combined with 200 uL 5 mg/ml dansyl chloride (Sigma Aldrich) in acetone and 100 uL saturated sodium bicarbonate. Samples were incubated in the dark overnight at room temperature. Excess dansyl chloride was cleared by incubating the reaction with 100 µL 150 mg/mL proline (Sigma Aldrich). Dansylated polyamines were extracted with 50 µL toluene (Sigma Aldrich) and centifuged. 5 µL of sample was added in small spots to the TLC plate (silica gel matrix; Sigma Aldrich) and exposed to ascending chromatography with 1:1 cyclohexane: ethylacetate. Plate was dried and visualized via exposure to UV.

Polyamine Luciferase Reporter Assay

To measure free polyamine levels in cells, a dual-luciferase vector containing the wild-type -1 frameshift antizyme OAZ1 (pC5730), kindly sent to us by Dr. Tom Dever from the National Institutes of Health, were transfected into cells with LipoD293 (SignaGen). Free polyamines modulate OAZ1 mRNA frameshifting and these constructs can measure relative endogenous polyamine concentrations via a dual-luciferase reporter as previously described (51) Huh7 cells were seeded with 2% media

and drug treated as described above. Cells were transfected with 62.5 ng of reporter plasmid of and after 24 hours of incubation, luminescent signal was measured using the Dual-Luciferase Reporter Assay System (Promega) by measuring both firefly and *Renilla* luciferase with the Veritas Microplate Luminometer (Turner Biosystems). Firefly luciferase was normalized to *Renilla* and the wild-type values and subsequently normalized to untreated controls.

Virus Preparation and Concentration

MP-12 was inoculation onto confluent Huh7 cells at an MOI of 0.001 and incubated for 48-72h, until full CPE. Supernatant was clarified via centrifugation and then concentrated using VivaSpin 20 centrifugal concentrators (GE Lifesciences). Virus was concentrated 1000-fold by resuspending in an appropriate amount of serum free DMEM.

RNA Purification and cDNA Synthesis

Media was cleared from cells and Trizol reagent (Zymo Research) directly added. Lysate was then collected, and RNA was purified according to the manufacturer's protocol utilizing the Direct-zol RNA Miniprep Plus Kit (Zymo Research). Purified RNA was subsequently used for cDNA synthesis using High Capacity cDNA Reverse Transcription Kits (Thermo-Fischer), according to the manufacturer's protocol, with 10-100 ng of RNA and random hexamer primers.

Viral Genome Quantification

Following cDNA synthesis, qRT-PCR was performed using the QuantStudio3 (Applied Biosystems by Thermo-Fischer) and SYBR green mastermix (DotScientific).

Samples were held at 95ºC for 2 mins prior to 40 cycles of 95ºC for 1s and 60ºC for 30s. Primer sequences are included in Table 1. Primers were verified for linearity using eight-fold serial diluted cDNA and checked for specificity via melt curve analysis following by agarose gel electrophoresis. All samples were used to normalize to total RNA using the ΔC_T method. Primer sequences are included in Table 1.

Table 1. Primers Utilized in This Study

Primers (qRT-PCR)	Forward	Reverse
MP12 - Small Segment	5'-CAGCAGCAACTCGTGATAGA-3'	5'-CCCGGAGGATGATGATGAAA-3'
MP12 - Medium Segment	5'-GGAACTAGGGAAGACTGAGAGA-3'	5'-CTGCTGAAGGGTGGAAACA-3'
MP12 - Large Segment	5'-CTCCACTAACCCAGAGATGATTG-3'	5'-CTCCTGGCTTGAGGTCTTAAC-3'
ZIKV	5'-CCCTCAAGTATAGCAGCAAGAG-3'	5'-TGAGTTGGAGTCCGGAAATG-3'
CVB3	5'-GGAAGCACGGGTCCAATAAA-3'	5'-CAGAGTCTAGGTGGTCTAGGTATC-3'
GAPDH	5’-GATTCCACCCATGGCAAATTC-3’	5’-CTGGAAGATGGTGATGGGATT-3’

Genome-to-PFU Ratio Calculations

The number of viral genomes quantified as described above were divided by the viral titer, as determined by plaque assay, to measure the genome-to-PFU ratio. Values obtained were normalized to untreated conditions to obtain the relative genome-to-PFU ratio.

Western Blot

Samples were collected with Bolt LDS Buffer and Bolt Reducing Agent (Invitrogen) and run on polyacrylamide gels. Gels were transferred using the iBlot 2 Gel Transfer Device (Invitrogen). Membranes were probed with primary antibodies for Rift Valley Fever nucleoprotein, N, glycoprotein N, G_N, (1:500, BEI Resources) and, β-actin (1:5000, Santa Cruz Biotechnology). Membranes were treated with SuperSignal West Pico PLUS Chemiluminescent Substrate (ThermoFisher Scientific) and visualized on ProteinSimple FluorChem E imager.

Silver Stain

Samples were collected with Bolt LDS Buffer and Bolt Reducing Agent (Invitrogen) and run on polyacrylamide gels. Gels were then washed with a fixative solution (50% methanol, 12% acetic acid, 0.05% formaldehyde) for 2 to 24 hours. After fixing, the gels were washed with a wash solution (35% ethanol) for 20 minutes and was repeated three times. Gels then were placed in a sensitizer solution (0.02% sodium thiolsulfate) for 5 minutes followed by 3 brief rinses with ddH_2O. Following the brief rinsing steps, the gels sat in a staining solution (0.2% silver nitrate, 0.076% formaldehyde) for 20 minutes. After the stain, the gels were washed with ddH_2O and the gels were revealed with developing solution (6% sodium carbonate, 0.05% formaldehyde, and 0.0004% sodium thiol sulfate) for 1 to 5 minutes. The reaction was then stopped with a stop solution (12% acetic acid) for 5 minutes and gels were stored in H_2O at 4ºC.

Indirect Immunofluorescence

Huh7 cells grown on cover slips were either treated with 500 μM DFMO or untreated. After four days cells were infected with MP12. Cells fixed with 4% formalin for 15 minutes, washed with PBS, permeabilized and blocked with 0.2% Triton X-100 and 2% BSA in PBS (blocking solution) for 30 minutes at room temperature (RT). Cells were sequentially incubated as follows: Primary mouse anti-Nucleoprotein antibody (1:100 in blocking solution, overnight at 4^{o}C), and secondary antibody, goat anti-mouse 488nm, (1:500 in PBS, 1hr, RT). Cells were then incubated in affinity pure Fab donkey anti-mouse IgG fragment (1:100 in blocking solution, Jackson ImmunoResearch, 1hr RT), followed by primary mouse anti-RNA (J2) antibody (1:100) and 633nm conjugated phalloidin (1:500) in blocking solution (overnight at 4^{o}C) and then secondary donkey anti-mouse 568nm (1:500 1hr at RT). After washing with PBS, cells were mounted with Invitrogen ProLong Diamond Antifade Mounting Media with DAPI for 30 min before imaging. To ensure that there was no binding of the 2nd fluorescent primary antibody to the first primary mouse antibody, control cells were processed as described above, but without the 2nd primary antibody step. Samples were imaged with Zeiss Axio Observer 7 with Lumencor Spectra X LED light system and a Hamamatsu Flash 4 camera using appropriate filters using Zen Blue software with a 40X objective.

Electron Microscopy

Concentrated Rift Valley Fever Virus (RVFV) samples were prepared for imaging by transmission electron microscopy according to a published method (Ellis et al., 1988) with minor modifications. Concentrated RVFV samples suspended in media were fixed

in 5% glutaraldehyde (Electron Microscopy Sciences, Hatfield, PA) for 24 h at room temperature. Fixed viral samples were subjected to ultracentrifugation then resuspended in 50 µl deionized water. Next, 5 µl of sample was pipetted onto a formvar- and carbon-coated 200 mesh copper grid (Electron Microscopy Sciences) held in place by negative-action tweezers. Five minutes later, the edge of the grid was blotted with a wedge of Whatman filter paper to remove excess sample. The sample was negatively stained by immersing the grid in a 1% solution of phosphotungstic acid (PTA) (pH 6.8) for 1 min. After the grid was removed from the 1% PTA solution, the edge of the grid was blotted with a wedge of Whatman filter paper, and the sample was allowed to air dry for 5 min. The sample was placed into a grid storage box and allowed to dry for 24 h prior to imaging with a Philips CM120 transmission electron microscope (TSS Microscopy, Beaverton, OR) equipped with a BioSprint 16 megapixel digital camera (Advanced Microscopy Techniques, Woburn, MA). (52)

Particle Size Measuring

We obtained images of viral particles via transmission electron microscopy (TEM) and negative staining. ImageJ was used to measure the diameter of the particles by measuring the provided standard from the TEM imaging software and measuring the particles which were then normalized to the standard.

Fractionation

Sucrose gradient ultracentrifugation was performed using an Optima L-90K ultracentrifuge with an SW60 Ti Beckman rotor and Ultra-Clear Centrifuge tubes (11x 60mm; Beckman Coulter). Varying densities of sucrose (20%-60%) was added to the

centrifuge tubes in 2.5% increments between 20% and 30% and 5% increments between 30% and 60%. Tubes were weighed before adding 50 ul to 200 ul of viral supernatant, unless otherwise indicated. Centrifuge tubes were then spun at 45,000 RPM for 18 hours at 4ºC. Samples were then collected based on fraction amount (450 uL) and analyzed by western blot, silver stain, and RT-qPCR.

Total Polyamine Assay

Huh7 cells were plated and either treated with 500 μM DFMO or untreated. After four days, cells were infected with MP12, VACV, and CVB3 at an MOI of 0.1 for 48 hours. Supernatant was collected. 20% sucrose was added to the centrifuge tube and tubes were weighed before adding 1mL of viral supernatant, unless otherwise indicated. Centrifuge tubes were then spun at 18,000 RPM for 1.5 hours at 4ºC. Pellets were then collected and Total Polyamine Assay Kit (BioVision Incorporated) was used and analyzed fluorescence of the whole sample with Synergy H1 microplate reader (BioTek).

Statistical Analysis

Prism 6 (GraphPad) was used to generate graphs and perform statistical analysis. For all analyses, one-tailed Student's t test was used to compare groups, unless otherwise noted, with $a = 0.05$. For tests of sample proportions, p values were derived from calculated Z scores with two tails and $a = 0.05$.

CHAPTER 3: RESULTS

RVFV is Sensitive to Polyamine Depletion.

Previous data focused on the role of polyamines in alphavirus and flavivirus replication (47). It was further demonstrated that polyamines are required for a number of distinct viral families (48). We understand little about potential roles for polyamines in these diverse viruses, however, to initially examine polyamines in RVFV replication, we sought to determine their sensitivity to polyamine depletion. DFMO at a concentration of 500 μM was sufficient to block alpha- and flavivirus replication(47, 48); thus, we investigated whether these parameters would similarly reduce RVFV infection (the vaccine strain of RVFV). We treated Huh7 cells with 500 μM DFMO for four days prior to infection at a multiplicity of infection (MOI) of 0.01 plaque-forming units (pfu) per cell with the vaccine strain of RVFV, MP-12. Samples were collected every eight hours and titered on Vero-E6 cells. We observed characteristic sigmoidal growth kinetics of untreated cells; however, DFMO-treated cells failed to produce virus (Figure 5A). In fact, viral titers remained flat over 64 hours of infection, suggesting that MP-12 failed to replicate without polyamines.

To measure sensitivity to DFMO and, thereby, polyamine depletion, we treated Huh7 cells with increasing doses of DFMO, from 100 μM to 5 mM and measured virus replication at 48 hours post infection (hpi) via plaque assay. We observed a significant decrease in titer when cells were treated with a minimum of 500 μM DFMO (Figure 5B). Both 1 mM and 5 mM treatments significantly reduced titers as well. We

verified that DFMO was depleting polyamines using a quantitative polyamine-sensitive luciferase assay (53), which demonstrated significant reductions in polyamine levels at all tested concentrations (Figure 5C). To visually confirm that these doses of DFMO were, in fact, depleting polyamines, we performed thin-layer chromatography (TLC) on polyamines. We found that, compared to untreated samples, DFMO treatment as low as 100 μM reduced polyamine levels and were undetectable at 500 μM (Figure 5D).

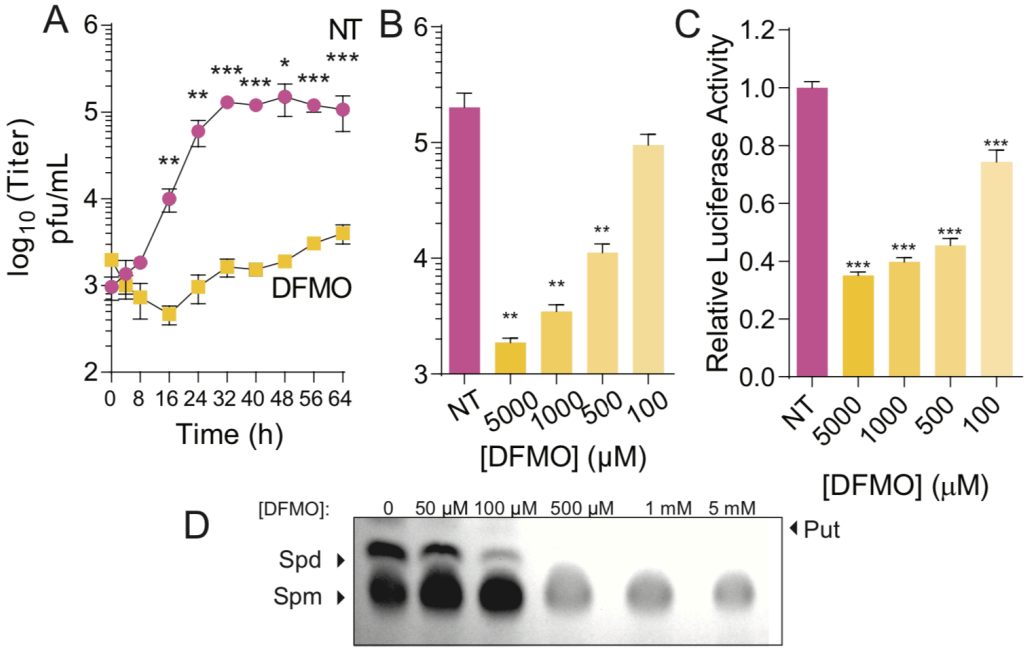

Figure 5. Rift Valley Fever Virus MP-12 is Sensitive to DFMO Treatment.
(A) Huh7 cells were left untreated or were treated with 500 μM DFMO for four days prior to infection at a multiplicity of infection (MOI) of 0.01 plaque-forming units of RVFV MP-12 strain per cell. Samples were collected every 8 h for 64 h and subsequently titered via plaque assay.
Huh7 cells were treated with escalating doses of DFMO as indicated and subsequently infected with (B) MP-12 at an MOI of 0.1 pfu per cell. Viral titers were determined at 48 h post infection.
(C) Intracellular polyamine levels were measured using a dual luciferase assay reporter of an OAZ1 transcript construct following DFMO treatment for four days. Relative luciferase activity was normalized to untreated samples.
(D) Thin layer chromatography on cells treated as in (B) to measure biogenic polyamine levels following DFMO treatment. *p ≤ 0.05, **p ≤ 0.01, ***p ≤ 0.001 using Student's t test (n ≥ 3) comparing untreated cells to DFMO treatment. Error bars represent ± 1 SEM. Statistical comparison were performed between treated and untreated conditions.

We next investigated whether MP-12 was sensitive to DENSpm. First, we performed a growth curve of MP-12 using 100 μM DENSpm, an activator of SAT1 which acetylates polyamines, leading to their neutralization and export from the cell (45, 46). We observed significant decreases in viral titers over a course of infection (Figure 6A). Using a range of DENSpm concentrations, we observed a decrease in MP-12 titers at concentrations greater than 50 μM (Figure 6B), similar to our data with other viruses (48). We confirmed via TLC and ImageJ quantitation of chromatogram that DENSpm reduced polyamine levels (Figure 6C and D).

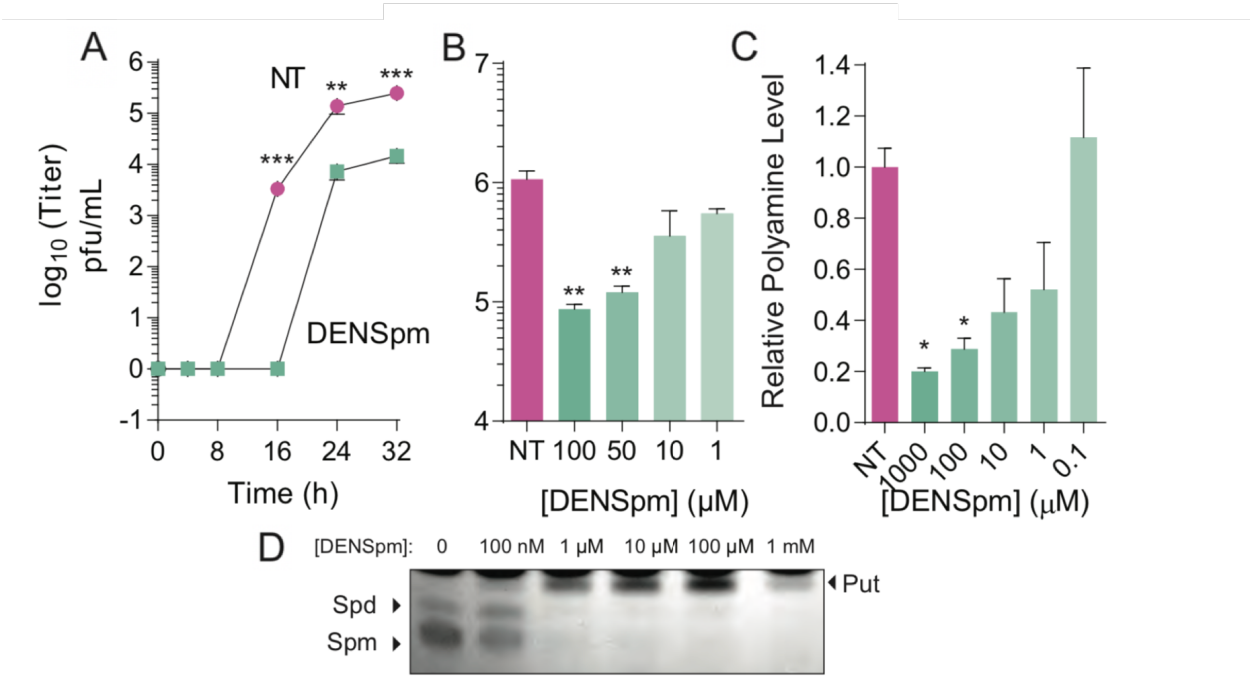

Figure 6. Rift Valley Fever Virus MP-12 is Sensitive to DENSpm Treatment.
(A) Huh7 cells were treated with 100 μM DENSpm for 16h prior to infection with MP-12 at an MOI of 0.01. Samples were collected every 8 h for 32 h and titered via plaque assay.
(B) Huh7 cells were treated with escalating doses of DENSpm as indicated and infected with MP-12 at an MOI of 0.01 pfu per cell. Viral titers were determined at 48 hpi.
(C) Relative polyamine levels as measured by thin layer chromatography (D) were quantified via ImageJ analysis and normalized to untreated controls. *p ≤ 0.05, **p ≤ 0.01, ***p ≤ 0.001 using Student's t test (n ≥ 3) comparing untreated cells to DFMO treatment. Error bars represent ± 1 SEM. Statistical comparison were performed between treated and untreated conditions.

RVFV Genome-to-PFU Ratio is Increased with Polyamine Depletion.

Reports have suggested that polyamines are present in the virions of diverse viruses and promote genome packaging (34, 35). We hypothesized that polyamines may function similarly for RVFV. To test whether polyamines are involved in RVFV packaging, we aimed to quantify the ratio of the number of genomes per virus in infected cell supernatant. To this end, we treated Huh7 cells with DFMO and subsequently infected with MP-12 at MOI 0.1 for 48h. We titered the virus and measured the number of genomes (small [S], medium [M], and large [L] segments) via quantitative Real Time-PCR (qRT-PCR) with genome-specific primers. As in Figure 5B, we observed reduced MP-12 titers with DFMO treatment (Figure 7A). We anticipated that if polyamines were involved in packaging, we would observe significantly fewer viral genomes in the infected cell supernatant. Surprisingly, we observed equivalent numbers of genomes in the supernatant with escalating doses of DFMO (Figure 7B). We next calculated the genome-to-PFU ratio by dividing the number of viral genomes by the titers (values in Figure 7B divided by 7A). We found a dramatic increase in the number of viral genomes per infectious virus in a DFMO dose-dependent manner (Figure 7C).

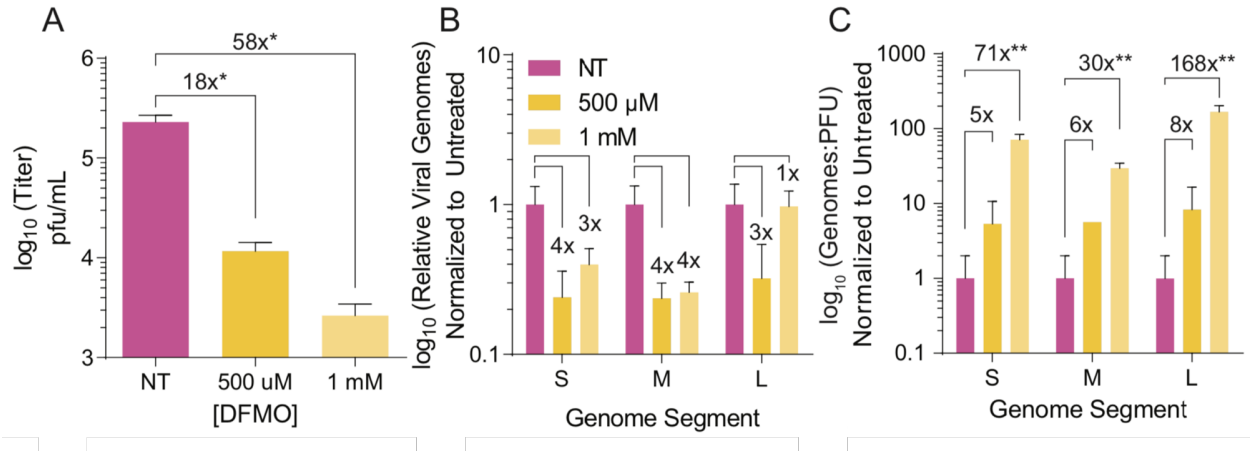

Figure 7. Specific Infectivity of RVFV MP-12 is Diminished with DFMO.
Huh7 cells were treated with either 500 µM or 1 mM DFMO for four days prior to infection with MP-12 at an MOI of 0.1 pfu per cell. (A) Viral titers were determined via plaque assay and (B) viral genomes in culture supernatant was quantified via qRT-PCR at 48 hpi. (C) The relative number of viral genomes from (B) was divided by the titer from (A) to determine the genome-to-pfu ratio, normalized to untreated controls. Values provided above data bars represent the fold change compared to untreated conditions. *p ≤ 0.05, **p ≤ 0.01, ***p ≤ 0.001 using Student's t test (n ≥ 3) comparing DFMO treatment to untreated controls. Error bars represent ± 1 SEM. Statistical comparison were performed between treated and untreated conditions.

We confirmed these phenotypes by depleting cells of polyamines with DENSpm. We treated cells with 10 or 100 µM DENSpm for 16h prior to infection at MOI 0.1. We collected and titered (Figure 8A) and measured genomes (Figure 8B) at 48 hpi. As with DFMO, MP-12 titers were decreased but viral genome levels were unchanged, resulting in high genome-to-PFU ratio (Figure 8C).

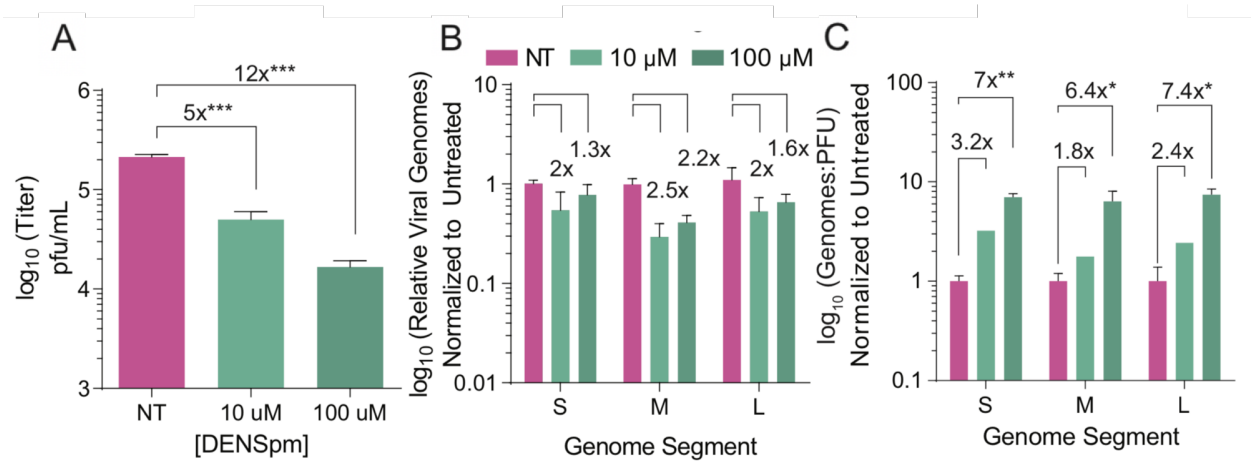

Figure 8. Specific Infectivity of RVFV MP-12 is Diminished with DENSpm.
Huh7 cells were treated with 10 or 100 μM DENSpm for 16h prior to infection with MP-12 at an MOI of 0.1 pfu per cell. (A) Viral titers were determined via plaque assay and (B) viral genomes quantified via qRT-PCR at 48 hpi. (C) The ratio of viral genomes (B) was divided by the titer from (A) to determine the genome-to-pfu ratio, normalized to untreated controls. Values provided above data bars represent the fold change compared to untreated conditions. *p ≤ 0.05, **p ≤ 0.01, ***p ≤ 0.001 using Student's t test (n ≥ 3) comparing DFMO treatment to untreated controls. Error bars represent ± 1 SEM. Statistical comparison were performed between treated and untreated conditions.

We next measured cell-associated viral RNA by extracting RNA from attached, infected cells. As with supernatant RNA, we observed no change in the number of genomes produced (Figure 9A). However, the MP-12 genomic RNA measurements could be free RNA or virion-associated RNA. To distinguish between the two, we treated our infected cell supernatant with RNAse A prior to genome quantification. We observed no change in the genome-to-PFU ratio with DFMO (Figure 9B), suggesting that a portion of supernatant genomic RNA was protected from RNAse degradation. We presume these RNAse-protected genomes are virion-associated; however, these data do not exclude the possibility that viral RNA could be contained in a vesicle or other layer to protect from degradation. This phenotype was confirmed again with DENSpm

treatment (Figure 9C). Together, these data suggest that polyamine-depleted cells have no defect in viral genome production or export.

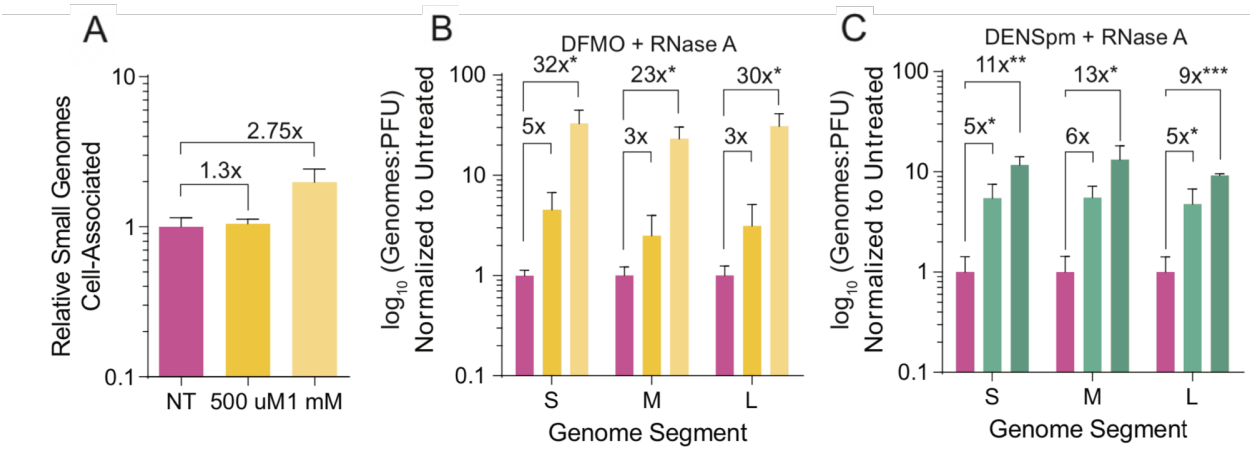

Figure 9. Specific Infectivity of RNAse Treated RVFV MP-12 is Diminished with Polyamine Depletion.
(A) Huh7 cells were treated and infected as in (Fig. 7 and Fig. 8) and the number of cell-associated viral genomes was determined via qRT-PCR, normalizing to cellular GAPDH.
(B,C) Samples from (Fig 7B) and (Fig 8B) were treated with RNase prior to genome quantification via qRT-PCR and divided by viral titers in (Fig 7A) and (Fig 8A) to determine the genome-to-pfu ratio. Values provided above data bars represent the fold change compared to untreated conditions. *$p \leq 0.05$, **$p \leq 0.01$, ***$p \leq 0.001$ using Student's t test ($n \geq 3$) comparing DFMO treatment to untreated controls. Error bars represent ± 1 SEM. Statistical comparison were performed between treated and untreated conditions.

RVFV Viral Protein Levels are Unchanged in Infected Cell Supernatant.

We observe that viral titers are reduced greater than 100-fold with DFMO treatment (Figure 5A and B). However, genome levels are unchanged relative to the control (Figure 7B). We hypothesized that this discrepancy could be due to aberrant virion protein content. To test this hypothesis, we measured the levels of N and G_N in both cells and infected cell supernatant. We observed no difference between the levels of viral proteins in the supernatant (Figure 10A), though there was a slight decrease in viral protein content when DFMO-treated intact cells were collected (Figure 10B).

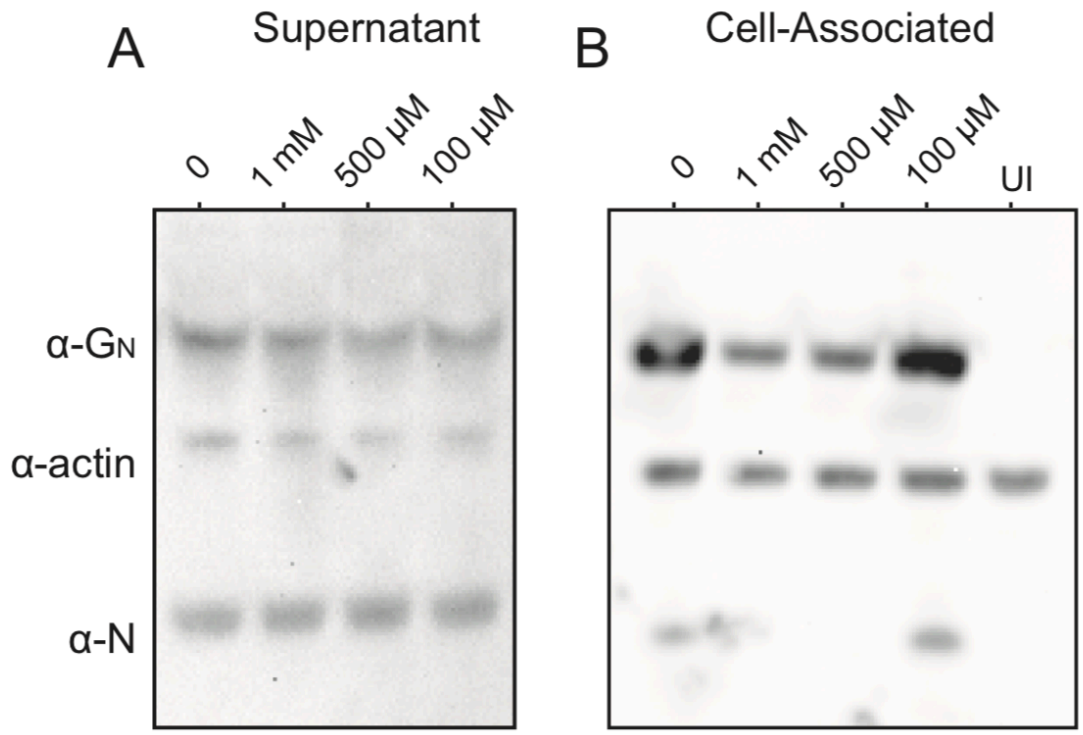

Figure 10. RVFV MP-12 Viral Protein Levels are Unchanged in Non-Cell Associated Virus Via Western Blot Analysis
Huh7 cells were treated with escalating doses of DFMO or left untreated for four days and subsequently infected at MOI of 0.1 pfu per cell or left uninfected. At 48 hpi, (A) supernatant and (B) cells were collected for western blot analysis for viral proteins G_N and N, as well as cellular GAPDH.

Because we observed significant changes in N protein levels in cell-associated protein but not in supernatant (Figure 10A and B), we investigated whether the N protein distribution changed with DFMO treatment. To this end, we imaged the N protein as well as double-stranded RNA (dsRNA, J2) in infected cells, either left untreated or treated with 500 μM DFMO. We noted that the N protein localized to perinuclear speckles that colocalized with dsRNA in both conditions (Figure 11). No significant detectable difference was noted between treatment conditions, though signal for the N protein was slightly reduced in DFMO treatment conditions, fitting with our observed western blot

results.

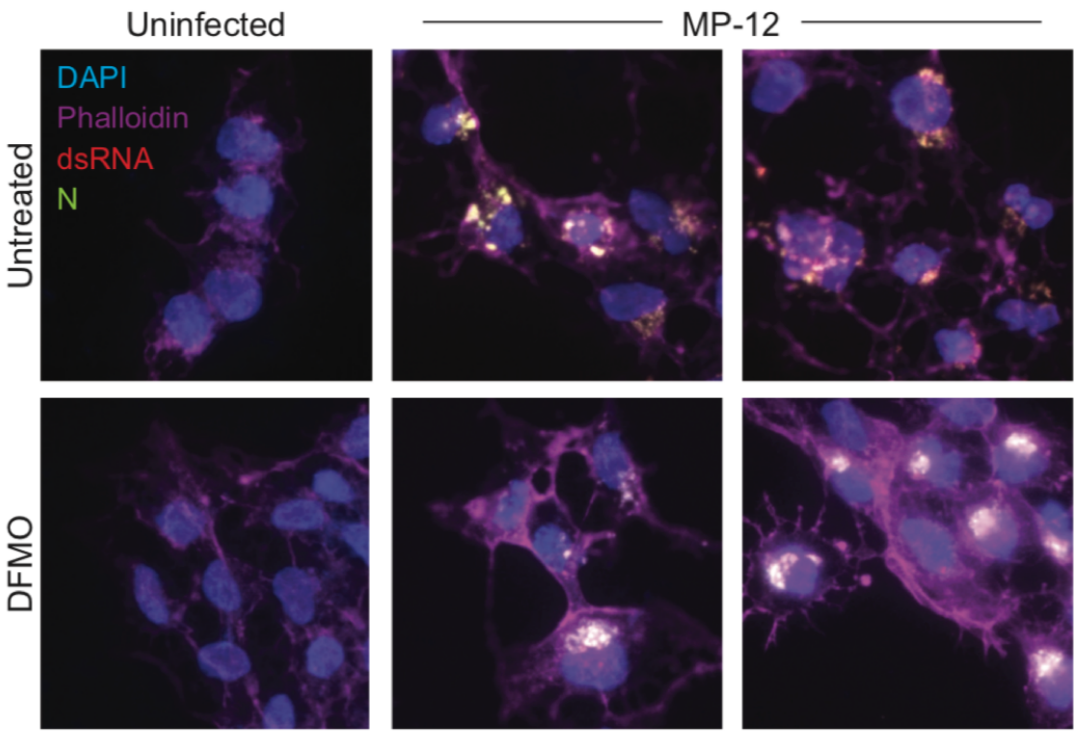

Figure 11. RVFV MP-12 Viral Protein Levels are Unchanged in Non-Cell Associated Virus Via Indirect Immunofluorescence
Huh7 cells were left untreated or treated with DFMO and infected with MP-12 for 48h prior to indirect immunofluorescence staining for nucleoprotein (N, green), double-stranded RNA (dsRNA, red), actin (purple), and nucleic acid (blue).

As an additional control, we measured global viral and cellular protein levels in infected cells and supernatants via silver stain gel to determine if a DFMO-modulated non-viral protein may contribute to infectivity. Again, we observed no gross differences in protein profiles on our silver stain gels, either in cells or in the supernatant (Figure 12A and B). These data suggest that DFMO does not alter viral protein levels in the infected cells supernatants.

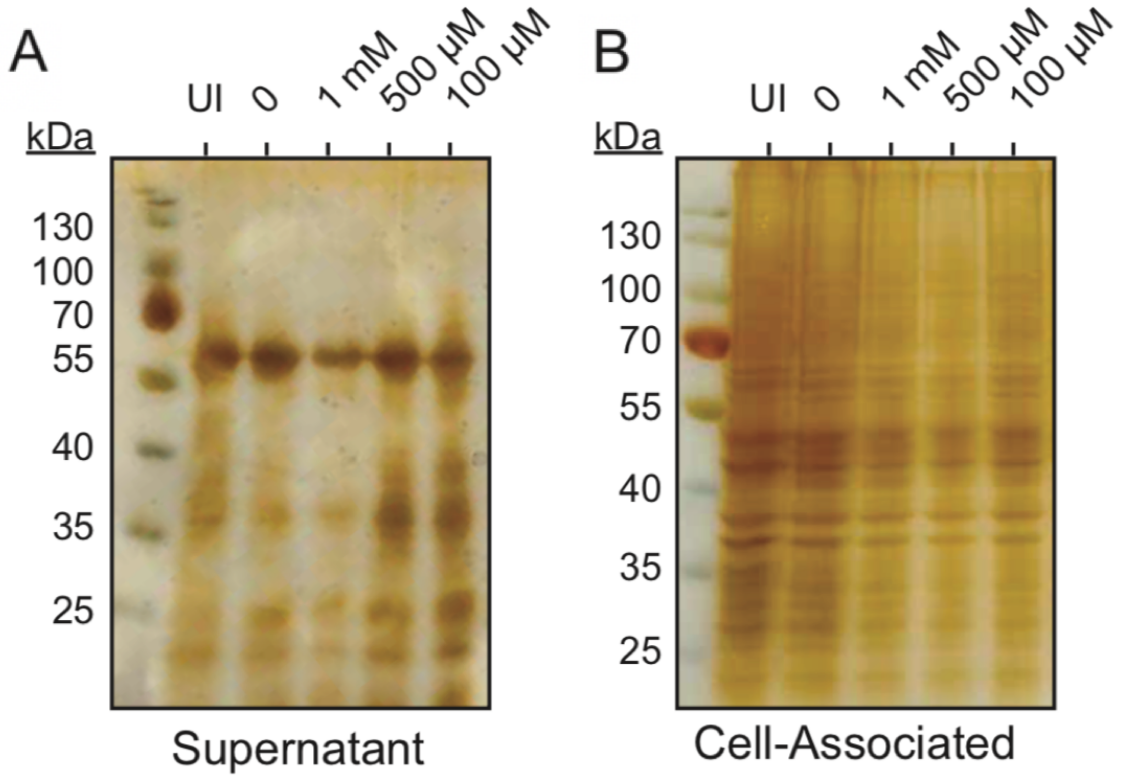

Figure 12. RVFV MP-12 Viral Protein Levels are Unchanged in Non-Cell Associated Virus Via Silver Stain Analysis
Samples from (Fig 10A) and (Fig 10B) were run on an acrylamide gel and analyzed for total protein content by silver stain for supernatant (A) and cell-associated (B) proteins.

Viral Particles from Polyamine-Depleted Cells Show No Significant Physical Differences.

We next sought to determine if polyamine depletion had any physical effect on the virions produced from infected cells. First, we generated viruses from untreated and DFMO-treated cells, concentrated and purified virions, and examined the particles by electron microscopy. We observed virions of size and shape previously described (Figure 13A) (52), with an average diameter of 90-110 nm. Intriguingly, we observed a similar number and size from virions derived from DFMO-treated cells (Figure 13B),

despite a lack of infectivity. These data suggest that fully formed viral particles are being produced but are not infectious.

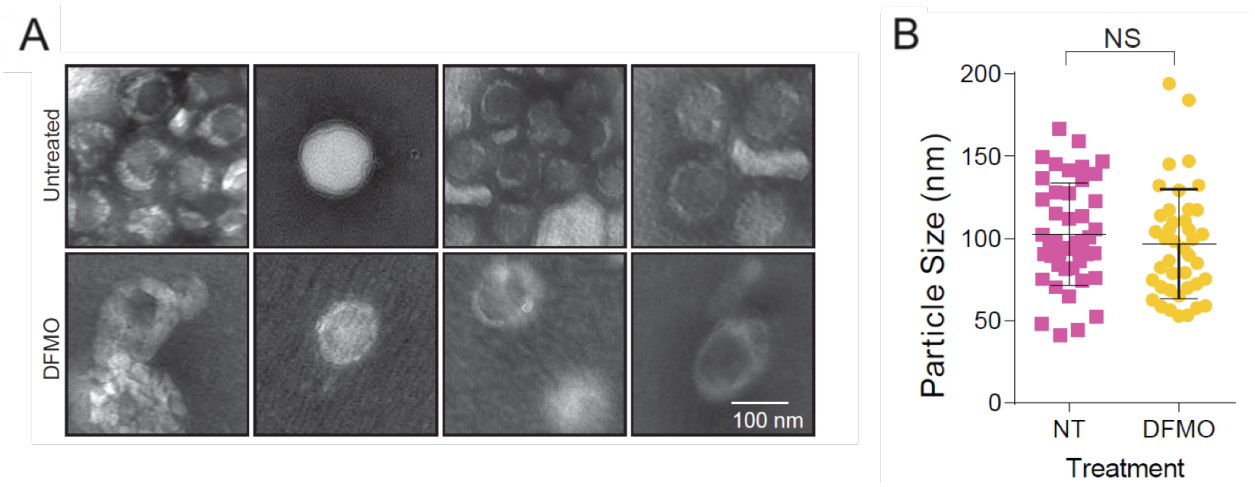

Figure 13. Physical Appearance of Secreted RVFV MP-12 Virions are Unchanged with Polyamine Depletion
(A) Huh7 cells were treated with 500 μM DFMO or left untreated and subsequently infected with MP-12 at MOI 0.1 pfu per cell for 48 h. Secreted viruses were collected, concentrated, and purified via ultracentrifugation prior to electron microscopy. Representative images are shown for each treatment condition.
(B) Diameter of viral particles derived from untreated or DFMO treated cells as in (A) were measured with ImageJ.

To determine whether polyamine depletion altered the buoyant properties of the MP-12 virions, we employed differential sucrose gradient ultracentrifugation. Using a 20-45% discontinuous gradient, we considered total protein content by silver staining the same fractions and observed viral proteins to a similar extent in both untreated and DFMO-treated conditions (Figure 14A), with peaks for these proteins in fractions from 22.5-30% sucrose. We observed MP-12 N protein in gradients ranging from 22.5-30% sucrose when analyzed by western blot, as previously described (50), for both virions from untreated and DFMO-treated cells. (Figure 14B). Viral genomes measured via qRT-PCR were also not statistically significantly different with polyamine depletion

(Figure 14C). We observed a peak in viral titers in these same fractions, though titers in DFMO treatment conditions were 10- to 100-fold lower (Figure 14D). In total, these results suggest that DFMO-mediated polyamine depletion does not alter the buoyant properties nor virion physical size, despite significant reductions in infectivity.

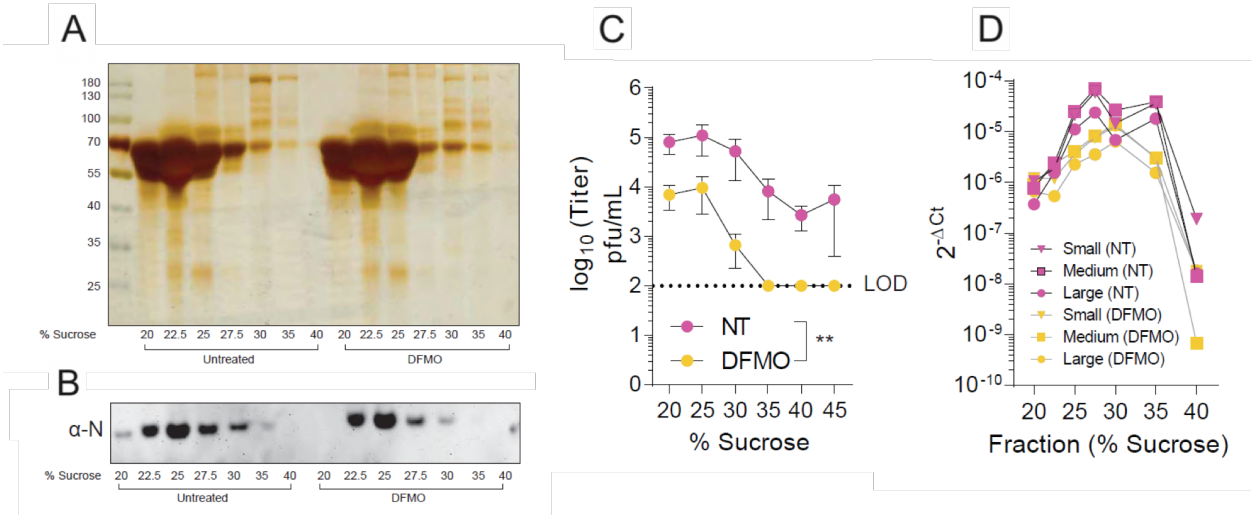

Figure 14. Physical Properties of Secreted RVFV MP-12 Virions are Unchanged with Polyamine Depletion
Huh7 cells were treated with 500 μM DFMO or left untreated and subsequently infected with MP-12 at MOI 0.1 pfu per cell for 48 h. Secreted viruses were collected, concentrated, and purified via ultracentrifugation. MP-12 particles were then subjected to discontinuous sucrose gradient ultracentrifugation, from 20% to 45% sucrose. Fractions were collected and analyzed by (A) silver stain, (B) western blot for viral N protein, (C) plaque assay to determine viral titers and (D) qRT-PCR to detect viral genomes. Error bars represent ± 1 SEM from n≥3.

Polyamines are Associated with RVFV MP-12 Virions

Polyamines are implicated in viral packaging for several different viruses (34–36). The positive charges of polyamines complement the negative charges of DNA/RNA backbone if the genome is to be packaged tightly, as it is in a compact virion. Certain DNA viruses contain enough polyamines within the virion to sufficiently neutralize 40%

of the negative charge of DNA (34, 35). It had been shown that RNA viruses encapsidate polyamines to a lesser extent than DNA viruses (29). Poliovirus, human rhinovirus 14, and encephalomyocarditis virus (EMCV) are viruses with reduced amounts of polyamines incorporated into mature virions (54, 55). The content of polyamines found was sufficient to neutralize 27% of the negative charge of RNA in rhinovirus 14, 11% in EMCV, and 1.6% in poliovirus (54, 55). Alternatively, myxoviruses, an RNA virus family including Newcastle disease virus (NDV) and influenza viruses, have been reported to encapsidate polyamines to neutralize around 30% of viral RNA (56). The variance in neutralization percent suggests that polyamines may contribute to viral packaging based on viral genome size and segment composition, as well as other poorly-defined factors. Poliovirus is a single stranded RNA virus while influenza is an 8 segmented RNA virus. RVFV having a tri-segmented genome may utilize polyamines for efficient packaging. To test this, we generated RVFV, Coxsackie B3 (CVB3, Nancy Strain), a single stranded RNA virus closely related to poliovirus(57), VACV, and ZIKV from untreated and DFMO-treated cells, subsequently concentrating and purifying the virions through ultracentrifugation. Pellets were collected, lysed and labeled for polyamines using a total polyamine assay kit which measures polyamine concentrations with fluorescence. In relation to the positive control (VACV) and negative control (CVB3), we observed that polyamines are associated with purified RVFV virions. In DFMO treated conditions, we see a reduction in polyamine fluorescence for all viruses including RVFV. We see no significant difference between untreated and DFMO treated

ZIKV, indicating that flaviviruses may not utilize polyamines in viral packaging; although data supports ZIKV uses polyamine in transcription and translation (48).

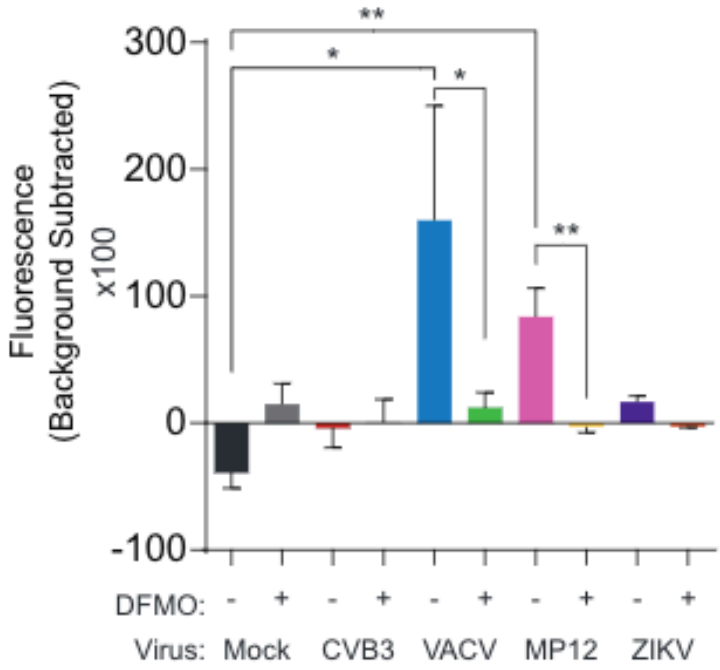

Figure 15. Polyamines are Associated with RVFV MP-12 Virions
Huh7 cells were treated with 500 μM DFMO or left untreated and subsequently infected with MP-12, CVB3, VACV, ZIKV and mock at MOI 0.1 pfu per cell for 48 h. Secreted viruses were collected, concentrated, and purified via ultracentrifugation. Pellets were collected, lysed, and labeled. Polyamine levels were measured using a total polyamine luciferase assay.

CHAPTER 4: DISCUSSION

Polyamines Play a Crucial Role in RVFV Infection

Our goal was to determine how polyamines may be involved in virus production and how they modulate RVFV infectivity. Because polyamines are ubiquitously found in all cells at high concentrations (58), it is likely that viruses like RVFV may have evolved a dependence on polyamines. While a role for polyamines in enzymatic activity of viral enzymes was previously uncovered (47), it was not determined whether polyamines were required for infectivity. Our data suggests that polyamines are crucial for the replication of RVFV and that polyamines promote infectivity of progeny virions through to-be-determined mechanism(s). Additionally, we reported that polyamines are crucial for other bunyaviruses including La Crosse virus (LACV) and Keystone virus (KEYV) (59). This study is the first to find that polyamines are required for infectivity of bunyaviruses. Both alphaviruses and flaviviruses were sensitive to polyamine depletion at the level of genome translation and RNA-dependent RNA polymerase activity (29); however, these prior studies had not investigated whether non-infectious particles were still produced from polyamine-depleted cells and whether polyamines potentially facilitate the encapsidation of viral genomes. Here, we have generated a working model whereby polyamines facilitate productive RVFV infection, and in the absence of polyamines, an altered ratio of genomes per infectious virus occurs causin noninfectious

particles to accumulate therefore reducing RVFV infection (Figure 16).

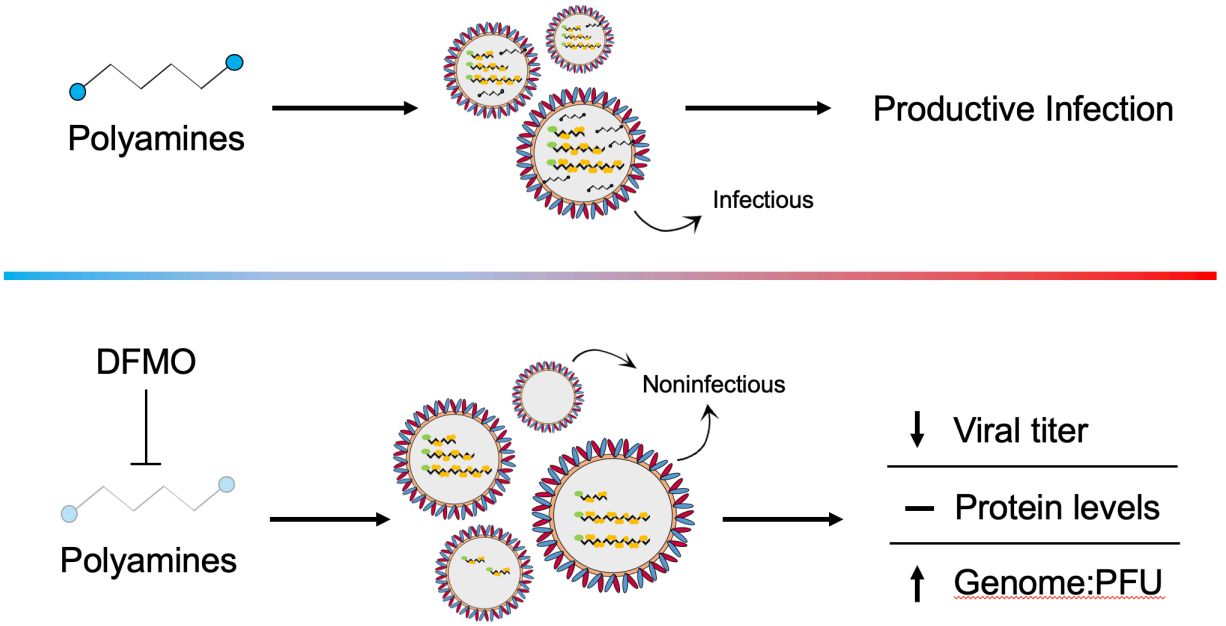

Figure 16. Proposed Model of RVFV MP-12 Infection With and Without Polyamines.
Cells containing polyamines support robust virus replication. In contrast, infection of polyamine depleted cells results in the accumulation of noninfectious viral particles that have an altered ratio of genomes per infectious virus and no change in viral protein levels. As a result, polyamine depletion limits RVFV replication.

Based on these data and others' previous data, polyamines play pleiotropic roles during viral infection (29). Due to their nature as small, abundant, positively-charged molecules, it is not surprising that they affect virus infection at distinct stages. Here, we find that for RVFV, polyamines are important for infectivity. With polyamine depletion, infected cells produce and export viral proteins and genomes, but the produced virions are non-infectious. Recent reports (59) demonstrated this phenotype did not hold true

for the non-enveloped CVB3, a positive-sense RNA virus. Enteroviruses like CVB3 are known to recombine to rapidly evolve (60), and this tendency to recombine may impede changes in the ratio of infectious to non-infectious virus. This defining feature of these distinct phenotypes deserve further investigation.

Polyamines Potentially Involved with RVFV Packaging

Genome packaging is an essential part of the viral life cycle. Previous work has established that several DNA viruses encapsidate significant concentrations of polyamines within the virion (34, 35), while several RNA viruses were found to contain insignificant amounts of polyamines (54, 55). In the case of herpesviruses, the viral genomes associate with histones in the nucleus (61–63) but are further neutralized by polyamines in the capsid. Vaccinia virus also utilizes polyamines to neutralize its genome to fold and package the viral DNA within the capsid (35). It is unclear whether this phenotype is a function of genome size and the need to neutralize a large amount of negatively-charged nucleic acid, versus a relatively smaller single-stranded RNA virus genome. Additionally, RNA viruses have evolved distinct packaging mechanisms that are not dependent on polyamines. The presence of polyamines in bunyavirus virions (or flavivirus or alphavirus virions) remains unexplored. Our data begins to address this idea that RVFV may utilize polyamines like VACV or HSV to neutralize its genome for establishing a persisting infection. It is not yet understood whether virion-bound polyamines affect infectivity or whether the virion stabilized by the polyamines and needs to be further characterized.

Polyamines Producing Defective Viral Particles

It is understood that most viruses do not possess proofreading mechanisms and are prone to high mutation rates(64). These mutations could therefore produce defective viral particles. These defective viral particles have received an increase in attention and appreciation for their novel roles in viral infection. Due to their inability to replicate independently, defective viral particles seize infectious viral (and cellular) machinery, reducing the capacity of the infectious virus to replicate (65). Several mechanisms have been described whereby RNA virus genomes become defective, via error-prone polymerases, unique RNA structures, or mistakes during viral genome replication (26). While attention has focused on how defective genomes attenuate the infectivity of viral particles, how cellular factors contribute to defective virus production is less clear. Our results suggest that polyamine depletion results in noninfectious virus generation but with fully intact virions. This could establish a novel role for polyamines where defective particles can establish an innate immune response. Mounce et al. previously uncovered a novel role for polyamines in the innate immune response via the polyamine-acetylating enzyme SAT1 (47). Upon interferon stimulation, SAT1 is induced and reduces polyamine pools within cells. Whether interferon-mediated polyamine depletion plays a role in generating defective virions from infection is an important hypothesis for future testing. In sum, our data suggests that the polyamine pathway is central to virus replication and reducing polyamine pools may effectively limit infection. Our results also suggest novel strategies to attenuate viruses: polyamine-depleted cells

produce fully assembled viruses that are non-infectious. Such an attenuation strategy may serve well to stimulate immune responses, which may function to enhance vaccine efficacy. While significant work remains, understanding how polyamines contribute to virus infectivity can provide insight into basic mechanisms of virus infectivity and highlight novel therapeutic routes.

REFERENCE LIST

1. Howard CR, Fletcher NF. 2012. Emerging virus diseases: can we ever expect the unexpected? Emerg Microbes Infect 1:e46.

2. NIAID Emerging Infectious Diseases/Pathogens | NIH: National Institute of Allergy and Infectious Diseases.

3. 2017. Bunyaviridae, p. 411–424. *In* Fenner's Veterinary Virology. Elsevier.

4. 2019. Outbreak Summaries | Rift Valley Fever | CDC.

5. WHO | Rift Valley fever – Kenya. WHO.

6. Daubney R, Hudson JR, Garnham PC. 1931. Enzootic hepatitis or rift valley fever. An undescribed virus disease of sheep cattle and man from east africa. J Pathol Bacteriol 34:545–579.

7. Himeidan YE, Kweka EJ, Mahgoub MM, El Rayah EA, Ouma JO. 2014. Recent Outbreaks of Rift Valley Fever in East Africa and the Middle East. Front Public Health 2.

8. Ahmad K. 2000. More deaths from Rift Valley fever in Saudi Arabia and Yemen. The Lancet 356:1422.

9. Linthicum KJ, Britch SC, Anyamba A. 2016. Rift Valley Fever: An Emerging Mosquito-Borne Disease. Annu Rev Entomol 61:395–415.

10. Tantely LM, Boyer S, Fontenille D. 2015. A Review of Mosquitoes Associated with Rift Valley Fever Virus in Madagascar. Am J Trop Med Hyg 92:722–729.

11. Mansfield KL, Banyard AC, McElhinney L, Johnson N, Horton DL, Hernández-Triana LM, Fooks AR. 2015. Rift Valley fever virus: A review of diagnosis and vaccination, and implications for emergence in Europe. Vaccine 33:5520–5531.

12. Sang R, Arum S, Chepkorir E, Mosomtai G, Tigoi C, Sigei F, Lwande OW, Landmann T, Affognon H, Ahlm C, Evander M. 2017. Distribution and abundance of key vectors of Rift Valley fever and other arboviruses in two ecologically distinct counties in Kenya. PLoS Negl Trop Dis 11.

13. Lumley S, Horton DL, Hernandez-Triana LLM, Johnson N, Fooks AR, Hewson R. 2017. Rift Valley fever virus: strategies for maintenance, survival and vertical transmission in mosquitoes. J Gen Virol 98:875–887.

14. McJunkin JE, Khan RR, Tsai TF. 1998. California-La Crosse encephalitis. Infect Dis Clin North Am 12:83–93.

15. Romero JR, Newland JG. 2003. Viral meningitis and encephalitis: Traditional and emerging viral agents. Semin Pediatr Infect Dis 14:72–82.

16. Schuffenecker I, Iteman I, Michault A, Murri S, Frangeul L, Vaney M-C, Lavenir R, Pardigon N, Reynes J-M, Pettinelli F, Biscornet L, Diancourt L, Michel S, Duquerroy S, Guigon G, Frenkiel M-P, Bréhin A-C, Cubito N, Desprès P, Kunst F, Rey FA, Zeller H, Brisse S. 2006. Genome Microevolution of Chikungunya Viruses Causing the Indian Ocean Outbreak. PLOS Med 3:e263.

17. Wikan N, Smith DR. 2016. Zika virus: history of a newly emerging arbovirus. Lancet Infect Dis 16:e119–e126.

18. Nishiyama S, Lokugamage N, Ikegami T. 2016. The L, M, and S Segments of Rift Valley Fever Virus MP-12 Vaccine Independently Contribute to a Temperature-Sensitive Phenotype. J Virol 90:3735–3744.

19. Faburay B, LaBeaud AD, McVey DS, Wilson WC, Richt JA. 2017. Current Status of Rift Valley Fever Vaccine Development. Vaccines 5:29.

20. Muyangwa M, Martynova EV, Khaiboullina SF, Morzunov SP, Rizvanov AA. 2015. Hantaviral Proteins: Structure, Functions, and Role in Hantavirus Infection. Front Microbiol 6.

21. Moutailler S, Roche B, Thiberge J-M, Caro V, Rougeon F, Failloux A-B. 2011. Host Alternation Is Necessary to Maintain the Genome Stability of Rift Valley Fever Virus. PLoS Negl Trop Dis 5.

22. Lowen AC, Boyd A, Fazakerley JK, Elliott RM. 2005. Attenuation of bunyavirus replication by rearrangement of viral coding and noncoding sequences. J Virol 79:6940–6946.

23. Alfson KJ, Avena LE, Beadles MW, Staples H, Nunneley JW, Ticer A, Dick EJ, Owston MA, Reed C, Patterson JL, Carrion R, Griffiths A. 2015. Particle-to-PFU Ratio of Ebola Virus Influences Disease Course and Survival in Cynomolgus Macaques. J Virol 89:6773–6781.

24. Mingozzi F, Anguela XM, Pavani G, Chen Y, Davidson RJ, Hui DJ, Yazicioglu M, Elkouby L, Hinderer CJ, Faella A, Howard C, Tai A, Podsakoff GM, Zhou S, Basner-Tschakarjan E, Wright JF, High KA. 2013. Overcoming preexisting humoral immunity to AAV using capsid decoys. Sci Transl Med 5:194ra92.

25. Patient R, Hourioux C, Roingeard P. 2009. Morphogenesis of hepatitis B virus and its subviral envelope particles. Cell Microbiol 11:1561–1570.

26. Rezelj VV, Levi LI, Vignuzzi M. 2018. The defective component of viral populations. Curr Opin Virol 33:74–80.

27. Xu J, Sun Y, Li Y, Ruthel G, Weiss SR, Raj A, Beiting D, López CB. 2017. Replication defective viral genomes exploit a cellular pro-survival mechanism to establish paramyxovirus persistence. Nat Commun 8:799.

28. Poirier EZ, Goic B, Tomé-Poderti L, Frangeul L, Boussier J, Gausson V, Blanc H, Vallet T, Loyd H, Levi LI, Lanciano S, Baron C, Merkling SH, Lambrechts L, Mirouze M, Carpenter S, Vignuzzi M, Saleh M-C. 2018. Dicer-2-Dependent Generation of Viral DNA from Defective Genomes of RNA Viruses Modulates Antiviral Immunity in Insects. Cell Host Microbe 23:353-365.e8.

29. Mounce BC, Olsen ME, Vignuzzi M, Connor JH. 2017. Polyamines and Their Role in Virus Infection. Microbiol Mol Biol Rev MMBR 81.

30. Gerner EW, Meyskens FL. 2004. Polyamines and cancer: old molecules, new understanding. Nat Rev Cancer 4:781–792.

31. Frugier M, Florentz C, Hosseini MW, Lehn JM, Giegé R. 1994. Synthetic polyamines stimulate in vitro transcription by T7 RNA polymerase. Nucleic Acids Res 22:2784–2790.

32. Mandal S, Mandal A, Johansson HE, Orjalo AV, Park MH. 2013. Depletion of cellular polyamines, spermidine and spermine, causes a total arrest in translation and growth in mammalian cells. Proc Natl Acad Sci U S A 110:2169–2174.

33. Brooks WH. 2013. Increased Polyamines Alter Chromatin and Stabilize Autoantigens in Autoimmune Diseases. Front Immunol 4.

34. Gibson W, Roizman B. 1971. Compartmentalization of spermine and spermidine in the herpes simplex virion. Proc Natl Acad Sci U S A 68:2818–2821.

35. Lanzer W, Holowczak JA. 1975. Polyamines in vaccinia virions and polypeptides released from viral cores by acid extraction. J Virol 16:1254–1264.

36. Tyms AS, Williamson JD. 1982. Inhibitors of polyamine biosynthesis block human cytomegalovirus replication. Nature 297:690.

37. Olsen ME, Cressey TN, Mühlberger E, Connor JH. 2018. Differential Mechanisms for the Involvement of Polyamines and Hypusinated eIF5A in Ebola Virus Gene Expression. J Virol 92.

38. Olsen ME, Filone CM, Rozelle D, Mire CE, Agans KN, Hensley L, Connor JH. 2016. Polyamines and Hypusination Are Required for Ebolavirus Gene Expression and Replication. mBio 7.

39. Bevec D, Jaksche H, Oft M, Wöhl T, Himmelspach M, Pacher A, Schebesta M, Koettnitz K, Dobrovnik M, Csonga R, Lottspeich F, Hauber J. 1996. Inhibition of HIV-1 Replication in Lymphocytes by Mutants of the Rev Cofactor eIF-5A. Science 271:1858.

40. Tuomi K, Raina A, Mäntyjärvi R. 1982. Synthesis of Semliki-forest virus in polyamine-depleted baby-hamster kidney cells. Biochem J 206:113–119.

41. Wallace HM, Fraser AV. 2004. Inhibitors of polyamine metabolism: Review article. Amino Acids 26:353–365.

42. Brun R, Schumacher R, Schmid C, Kunz C, Burri C. 2001. The phenomenon of treatment failures in Human African Trypanosomiasis. Trop Med Int Health 6:906–914.

43. Fabian CJ, Kimler BF, Brady DA, Mayo MS, Chang CHJ, Ferraro JA, Zalles CM, Stanton AL, Masood S, Grizzle WE, Boyd NF, Arneson DW, Johnson KA. 2002. A phase II breast cancer chemoprevention trial of oral alpha-difluoromethylornithine: breast tissue, imaging, and serum and urine biomarkers. Clin Cancer Res Off J Am Assoc Cancer Res 8:3105–3117.

44. Simoneau AR, Gerner EW, Nagle R, Ziogas A, Fujikawa-Brooks S, Yerushalmi H, Ahlering TE, Lieberman R, McLaren CE, Anton-Culver H, Meyskens FL. 2008. The effect of difluoromethylornithine on decreasing prostate size and polyamines in men: results of a year-long phase IIb randomized placebo-controlled chemoprevention trial. Cancer Epidemiol Biomark Prev Publ Am Assoc Cancer Res Cosponsored Am Soc Prev Oncol 17:292–299.

45. Goyal L, Supko JG, Berlin J, Blaszkowsky LS, Carpenter A, Heuman DM, Hilderbrand SL, Stuart KE, Cotler S, Senzer NN, Chan E, Berg CL, Clark JW, Hezel AF, Ryan DP, Zhu AX. 2013. Phase 1 study of N(1),N(11)-diethylnorspermine (DENSPM) in patients with advanced hepatocellular carcinoma. Cancer Chemother Pharmacol 72:1305–1314.

46. Wolff AC, Armstrong DK, Fetting JH, Carducci MK, Riley CD, Bender JF, Casero RA, Davidson NE. 2003. A Phase II study of the polyamine analog N1,N11-diethylnorspermine (DENSpm) daily for five days every 21 days in patients with previously treated metastatic breast cancer. Clin Cancer Res Off J Am Assoc Cancer Res 9:5922–5928.

47. Mounce BC, Poirier EZ, Passoni G, Simon-Loriere E, Cesaro T, Prot M, Stapleford KA, Moratorio G, Sakuntabhai A, Levraud J-P, Vignuzzi M. 2016. Interferon-Induced Spermidine-Spermine Acetyltransferase and Polyamine Depletion Restrict Zika and Chikungunya Viruses. Cell Host Microbe 20:167–177.

48. Mounce BC, Cesaro T, Moratorio G, Hooikaas PJ, Yakovleva A, Werneke SW, Smith EC, Poirier EZ, Simon-Loriere E, Prot M, Tamietti C, Vitry S, Volle R, Khou C, Frenkiel M-P, Sakuntabhai A, Delpeyroux F, Pardigon N, Flamand M, Barba-Spaeth G, Lafon M, Denison MR, Albert ML, Vignuzzi M. 2016. Inhibition of Polyamine Biosynthesis Is a Broad-Spectrum Strategy against RNA Viruses. J Virol 90:9683–9692.

49. Raina A, Tuomi K, Mäntyjärvi R. 1981. Roles of polyamines in the replication of animal viruses. Med Biol 59:428–432.

50. Ikegami T, Won S, Peters CJ, Makino S. 2006. Rescue of infectious rift valley fever virus entirely from cDNA, analysis of virus lacking the NSs gene, and expression of a foreign gene. J Virol 80:2933–2940.

51. Ivanov IP, Shin B-S, Loughran G, Tzani I, Young-Baird SK, Cao C, Atkins JF, Dever TE. 2018. Polyamine Control of Translation Elongation Regulates Start Site Selection on Antizyme Inhibitor mRNA via Ribosome Queuing. Mol Cell 70:254-264.e6.

52. Ellis DS, Shirodaria PV, Fleming E, Simpson DIH. 1988. Morphology and development of Rift Valley fever virus in vero cell cultures. J Med Virol 24:161–174.

53. Ivanov IP, Shin B-S, Loughran G, Tzani I, Young-Baird SK, Cao C, Atkins JF, Dever TE. 2018. Polyamine Control of Translation Elongation Regulates Start Site Selection on Antizyme Inhibitor mRNA via Ribosome Queuing. Mol Cell 70:254-264.e6.

54. Fout GS, Medappa KC, Mapoles JE, Rueckert RR. 1984. Radiochemical determination of polyamines in poliovirus and human rhinovirus 14. J Biol Chem 259:3639–3643.

55. Sheppard SL, Burness AT, Boyle SM. 1980. Polyamines in encephalomyocarditis virus. J Virol 34:266–267.

56. Bachrach U, Don S, Wiener H. 1974. Occurrence of Polyamines in Myxoviruses. J Gen Virol 22:451–454.

57. van der Linden L, Wolthers KC, van Kuppeveld FJM. 2015. Replication and Inhibitors of Enteroviruses and Parechoviruses. Viruses 7:4529–4562.

58. Igarashi K, Kashiwagi K. 2000. Polyamines: Mysterious Modulators of Cellular Functions. Biochem Biophys Res Commun 271:559–564.

59. Mastrodomenico V, Esin JJ, Graham ML, Tate PM, Hawkins GM, Sandler ZJ, Rademacher DJ, Kicmal TM, Dial CN, Mounce BC. 2019. Polyamine depletion inhibits bunyavirus infection via generation of noninfectious interfering virions. J Virol JVI.00530-19.

60. Xiao Y, Rouzine IM, Bianco S, Acevedo A, Goldstein EF, Farkov M, Brodsky L, Andino R. 2016. RNA Recombination Enhances Adaptability and Is Required for Virus Spread and Virulence. Cell Host Microbe 19:493–503.

61. Kent JR, Zeng P-Y, Atanasiu D, Gardner J, Fraser NW, Berger SL. 2004. During lytic infection herpes simplex virus type 1 is associated with histones bearing modifications that correlate with active transcription. J Virol 78:10178–10186.

62. Mounce BC, Tsan FC, Kohler S, Cirillo LA, Tarakanova VL. 2011. Dynamic association of gammaherpesvirus DNA with core histone during de novo lytic infection of primary cells. Virology 421:167–172.

63. Oh J, Fraser NW. 2008. Temporal association of the herpes simplex virus genome with histone proteins during a lytic infection. J Virol 82:3530–3537.

64. Sanjuán R, Nebot MR, Chirico N, Mansky LM, Belshaw R. 2010. Viral Mutation Rates. J Virol 84:9733–9748.

65. Manzoni TB, López CB. 2018. Defective (interfering) viral genomes re-explored: impact on antiviral immunity and virus persistence. Future Virol 13:493–503.

VITA

The author, Vincent Mastrodomenico, was born in Elk Grove Village, Illinois on July 26th, 1994 to Jill and Pat Mastrodomenico. He attended St. Norbert College in De Pere, Wisconsin where he earned a Bachelor of Science in Biology.

He matriculated to Loyola University Chicago in July 2017, in the Microbiology & Immunology MS program. He joined the lab of Dr. Bryan Mounce where he helped investigate the importance of cellular molecules called polyamines for bunyavirus infection. After completion of his graduate studies, Vincent will continue to work at the bench as a Research Associate II under the continued supervision of Dr. Bryan Mounce in hopes of pursuing a career in medicine.